Measurement and reduction of EMI radiated by a PWM inverter-fed AC motor drive system

Satoshi Ogasawara   Hideki Ayano
Okayama University   Okayama University

Hirofumi Akagi
Okayama University

Measurement and Reduction of EMI Radiated by a PWM Inverter-Fed AC Motor Drive System

Satoshi Ogasawara, *Senior Member, IEEE,* Hideki Ayano, and Hirofumi Akagi, *Fellow, IEEE*

Abstract—**This paper presents theoretical and experimental relationships between radiated electromagnetic noises and common-mode and normal-mode currents, paying attention to an induction motor drive system fed by a voltage-source pulsewidth modulation (PWM) inverter. A method of reducing both currents is proposed, based on an equivalent model, taking into account parasitic stray capacitors inside an induction motor. Electromagnetic interference (EMI) radiated by a 3.7-kW induction motor drive system is actually measured, complying with the VDE 0871 Class A [3 m]. Experimental results verify that the combination of the already proposed common-mode transformer (CMT) and the normal-mode filters (NMF's) being proposed in this paper is a practically viable and effective way to reduce EMI resulting from both common-mode and normal-mode currents.**

Index Terms—Common-mode transformer, electromagnetic interference (EMI), normal-mode filter.

TABLE I
TESTED INVERTER AND INDUCTION MOTOR RATINGS

rated voltage	3ϕ 200	V
rated current	21.0	A
maximum current	52.0	A
modulation scheme	sinusoidal PWM	
carrier frequency	2.4	kHz
rated output	3.7	kW
rated torque	23.5	Nm
maximum torque	70.6	Nm
motor speed	1500/2000	r/min

I. INTRODUCTION

THE PROGRESS of high-speed switching devices such as insulated gate bipolar transistors (IGBT's) has enabled us to increase the carrier frequency of voltage-source pulsewidth modulation (PWM) inverters, thus, leading to much better operating characteristics. Accompanying high-speed switching, however, are the following problems originating from a step voltage/current change:

- ground current escaping to earth through stray capacitors inside motors [1], [2];
- conducted and radiated electromagnetic interference (EMI) [3]–[5];
- bearing current and shaft voltage [6], [7];
- shortening of insulation life of motors and transformers [8]–[11].

The step change in voltage/current caused by high-speed switching produces high-frequency oscillatory common-mode and normal-mode currents at the instant of every switching,

because parasitic stray capacitors inevitably exist inside an ac motor. The oscillatory currents with a frequency range of 100 kHz to several megahertz can create a magnetic field, and radiate EMI noises throughout, thus, having a bad effect on electronic devices such as AM radio receivers and medical equipment. However, little has been reported in the literature on radiated EMI by power electronic equipment.

This paper presents theoretical and experimental relationships between radiated EMI noise and the high-frequency oscillatory common-mode and normal-mode currents, paying attention to an induction motor drive system fed by a voltage-source PWM inverter. A method of reducing both currents is proposed, based on a motor model taking into account parasitic stray capacitors inside an induction motor. The common-mode current oscillation can be perfectly damped by the common-mode transformer (CMT) which has been proposed by the authors [2], while the normal-mode current oscillation can be damped by the normal-mode filters (NMF's) being proposed in this paper. The EMI radiated by a 3.7-kW induction motor drive system is actually measured, complying with the VDE 0871 Class A [3 m].

Experimental results verify that the combination of the CMT and the NMF's is a practically viable and effective way to reduce EMI resulting from both common-mode and normal-mode currents.

II. SYSTEM CONFIGURATION

Fig. 1 shows the configuration of an experimental system. An induction motor of 3.7 kW is driven by a voltage-source PWM inverter through three feeding wires. The motor frame is connected to a virtual grounding point through a grounding wire. Four 10-m-long copper wires in cross-sectional area of 5.5 mm^2 are used for the three feeding wires and the grounding wire. Table I shows the experimental inverter and induction motor ratings.
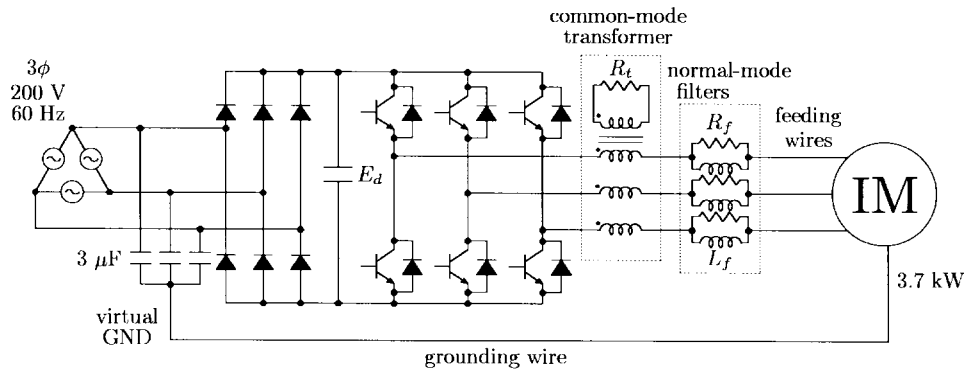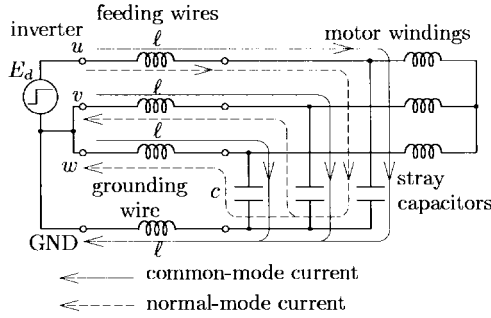
Fig. 1.   System configuration.

Fig. 2.   Motor model including stray capacitors.

TABLE II
COMMON-MODE AND NORMAL-MODE

item	L	C	E	Z	ω
common-mode	$\dfrac{4}{3}\ell$	$3c$	$\dfrac{1}{3}E_d$	$\dfrac{2}{3}\sqrt{\ell/c}$	$\dfrac{1}{2}\dfrac{1}{\sqrt{\ell c}}$
normal-mode	$\dfrac{3}{2}\ell$	$\dfrac{2}{3}c$	E_d	$\dfrac{3}{2}\sqrt{\ell/c}$	$\dfrac{1}{\sqrt{\ell c}}$
ratio $\left(\dfrac{\text{common}}{\text{normal}}\right)$	$\dfrac{8}{9}$	$\dfrac{9}{2}$	$\dfrac{1}{3}$	$\dfrac{4}{9}$	$\dfrac{1}{2}$

L: inductance Z: characteristic impedance
C: capacitance ω: resonant frequency
E: voltage

A CMT and three NMF's are connected to the inverter output terminals. The CMT is the same as a conventional common-mode choke, except for adding a secondary winding shorted by a resistor R_t, intended for damping of the common-mode current oscillation [2]. Each normal-mode filter consists of parallel connection of an inductor L_f and a resistor R_f, intended for damping of the normal-mode current oscillation. The common-mode current dissipates a small amount of active power in R_t, while the normal-mode current dissipates a negligible amount of active power in R_f.

A virtual grounding point is introduced to avoid the influence of an internal impedance between the earth terminal on the switch board and the actual grounding point [2]. Three capacitors, with a capacitance value being much larger than the stray capacitance in the motor, are connected to the three-phase ac terminals of the diode rectifier. The grounding wire is connected to the neutral point of the three capacitors, which is considered a virtual grounding point. In the experimental system, the capacitors of 3 μF are used for providing the virtual grounding point.

III. COMMON-MODE AND NORMAL-MODE CURRENTS

Fig. 2 shows a motor model taking the stray capacitors inside the motor into account [2]. The stray capacitors are represented by three capacitors in the motor model c. The stray capacitor between a stator winding and the motor frame has a capacitance value larger than that between two stator windings, because the stator windings are embedded into slots of the stator core. Accordingly, any stray capacitance between two

stator windings is negligible. Here, ℓ means a line inductance of each feeding wire between the inverter and motor terminals.

Moreover, Fig. 2 corresponds to the case of switching from the lower to the upper potential of the dc link voltage, when the other two phases remain connected to the lower potential. Note that the GND terminal is connected to the lower potential, based on the following assumptions.

- The high-frequency common-mode impedance of the diode rectifier is negligible.
- The grounding wire and the feeding wires have a line inductor with the same inductance value.

After the switching, the dc-link voltage E_d is applied only to the u-phase terminal, thus, increasing the common-mode voltage by $E_d/3$. Once a switching occurs in one phase of the inverter, a common-mode current and a normal-mode current can flow, which are depicted by the solid line and the broken line, respectively, shown in Fig. 2. The common-mode current is also referred to as the zero-sequence current or the ground current escaping through the stray capacitors to the grounding wire. The normal-mode current flows from one phase, in which a switching occurs, to the other two phases through the stray capacitors.

The inductance and capacitance concerning the common-mode current, shown as the solid line in Fig. 2, are $L_c = \frac{4}{3}\ell$ and $C_c = 3c$, respectively. On the other hand, the circuit loop for the normal-mode current, shown as the broken line, has an inductance of $L_n = \frac{3}{2}\ell$ and a capacitance of $C_n = \frac{2}{3}c$. Table II summarizes the circuit parameters which have relation
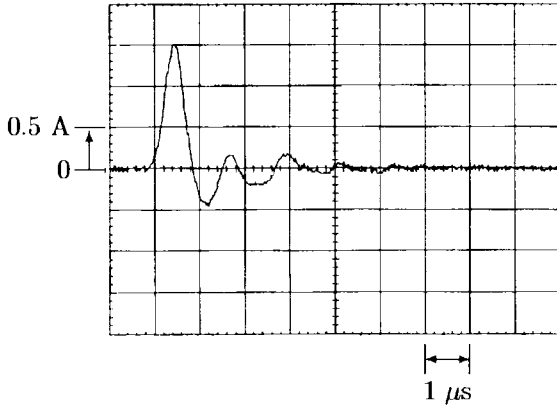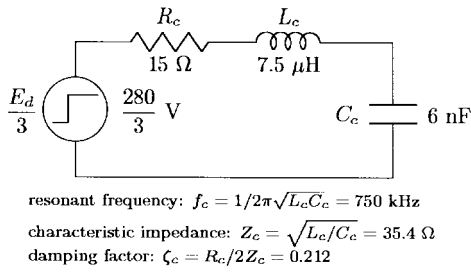
Fig. 3. Common-mode current waveform without CMT.

resonant frequency: $f_c = 1/2\pi\sqrt{L_c C_c} = 750$ kHz

characteristic impedance: $Z_c = \sqrt{L_c/C_c} = 35.4$ Ω

damping factor: $\zeta_c = R_c/2Z_c = 0.212$

Fig. 4. Equivalent circuit for common-mode current.

Fig. 5. CMT.

Fig. 6. Equivalent circuit for common-mode current when connected with CMT.

to the common-mode and normal-mode currents. The ratios of voltage, characteristic impedance, and resonant frequency can be calculated as 1/3, 4/9, and 1/2, respectively. This implies that the normal-mode current has the amplitude three-fourths times as large as the common-mode current and has the oscillatory frequency twice as high as the common-mode current.

IV. CMT

Fig. 3 shows a measured waveform of the common-mode current or the ground current that flows through the grounding wire, when a switching occurs in a phase of the PWM inverter. Neither the CMT nor the NMF's are connected in Fig. 3. A nonnegligible amount of common-mode current flows through the stray capacitors, which has a peak value of 1.5 A with an oscillation frequency of 750 kHz under the rated motor current of 21.0 A.

Fig. 4 shows an equivalent circuit for the common-mode current, which forms an *LCR* series resonant circuit. A switching in one phase causes a step change of the common-mode voltage by 1/3 of the dc-link voltage. The circuit parameters are estimated from the experimental waveform shown in Fig. 3, considering a rise time of 340 ns in the inverter output voltage.

In order to reduce the common-mode current, the CMT proposed by the authors [2] is connected to the inverter output terminals. The CMT is the same as a conventional common-mode choke except for adding a tightly coupled secondary winding, the terminals of which are shorted by a resistor.
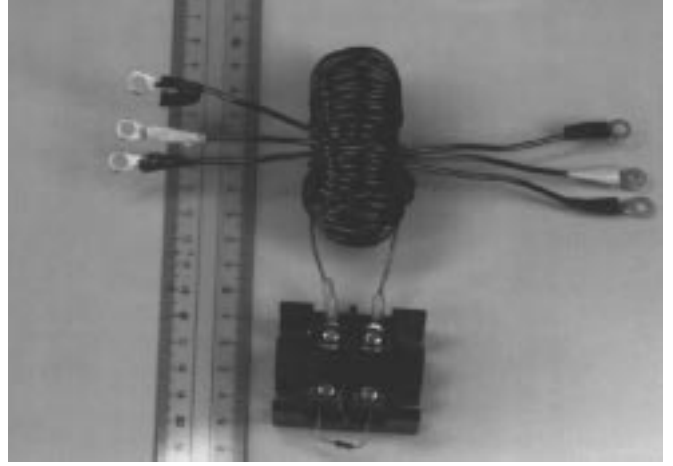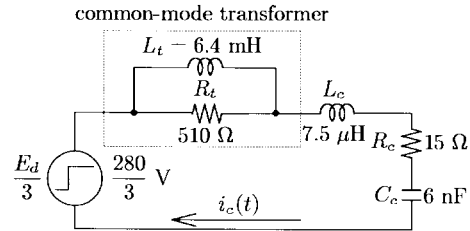
Although the common-mode current flowing in the three-phase feeding wires produces a flux in the ferrite core, no flux is created by the remaining inverter output current. Therefore, the CMT acts as a damping resistor only for the common-mode current, i.e., the ground current.

According to the already proposed design method [2], a prototype CMT was designed and built for the experimental system. Fig. 5 shows a photograph of the CMT. A damping resistor of 0.5 W is connected to the secondary winding terminals, because a negligible amount of power would be dissipated in the resistor. Fig. 6 shows the equivalent circuit for the common-mode current when connected with the CMT. Because its leakage inductance is negligible, the CMT is represented by a magnetizing inductor connected in parallel with the damping resistor. The inductance and resistance values are 6.4 mH and 510 Ω, respectively.

Fig. 7 shows a measured waveform of the common-mode current with the CMT connected. Comparing Fig. 7 with Fig. 3, we see that the peak value of the common-mode current is reduced to 1/8 and, also, that perfect damping of the common-mode current oscillation is achieved by the CMT.

V. NMF's

Fig. 8 shows a measured waveform of the inverter output current in a phase at the moment a switching occurs in the corresponding phase. A nonnegligible amount of the normal-mode current is superimposed on the motor current along with 1/3 of the common-mode current, as shown in Fig. 3.
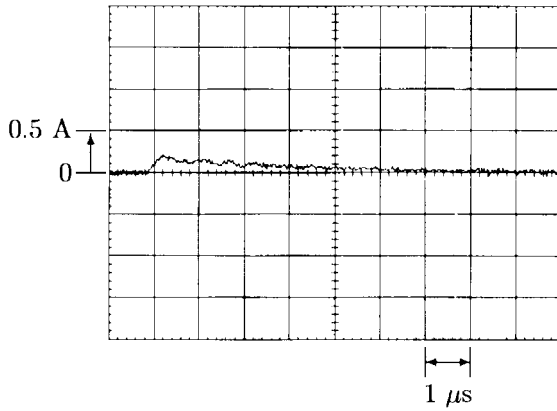
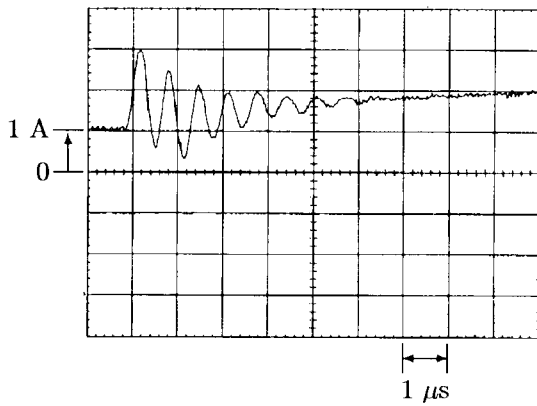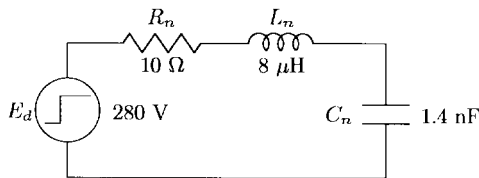Fig. 7.   Common-mode current waveform when connected with CMT.

Fig. 8.   Inverter output current waveform superimposing normal-mode current on motor current, without NMF's.

resonant frequency: $f_n = 1/2\pi\sqrt{L_n C_n} = 1.50$ MHz

characteristic impedance: $Z_n = \sqrt{L_n/C_n} = 75.6\ \Omega$

damping factor: $\zeta_n = R_n/2Z_n = 0.066$

Fig. 9.   Equivalent circuit for normal-mode current.

The oscillatory component or the normal-mode current in the inverter output current has a peak value of 2 A and an oscillatory frequency of 1.5 MHz. Hence, the normal-mode current may not only cause EMI, but also ringing and overvoltage at the motor terminals. Comparing the normal-mode current oscillation with the common-mode current oscillation leads to the fact that the peak value and oscillation frequency ratios are 4/3 and 2, respectively. The experimental results agree with the analytical results shown in Table II.

Fig. 9 shows an equivalent circuit for the normal-mode current, which forms an *LCR* series resonant circuit. A switching in one phase causes a step change of the normal-mode voltage by the dc-link voltage. Like the circuit parameters in the
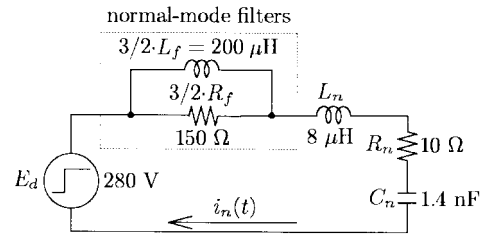

Fig. 10.   Equivalent circuit for normal-mode current when connected with NMF's.

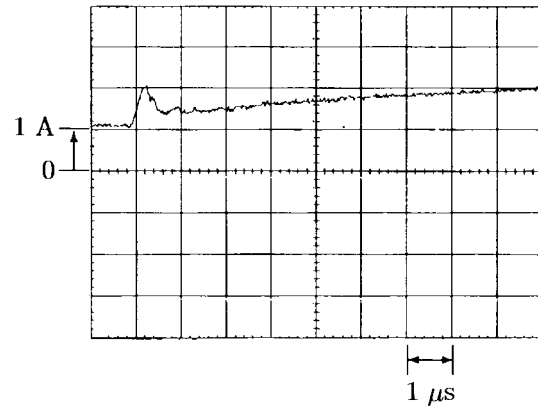Fig. 11.   Normal-mode filter inductor used for experiment.

Fig. 12.   Inverter output current waveform when connected with NMF's.

common-mode equivalent circuit, those in Fig. 9 are estimated from the experimental waveform shown in Fig. 8, considering a rise time of the inverter output voltage of 340 ns.

Comparing these circuit values with those in the Fig. 4, the inductance ratio $L_c/L_n = 0.94$ and the capacitance ratio $C_c/C_n = 4.3$ also approximate 8/9 and 9/2, as shown in Table II, respectively. This verifies that the motor model of Fig. 2 is capable of dealing with both common-mode and normal-mode currents.

In order to damp the normal-mode current oscillation, a resistor has to be inserted in series with the normal-mode current loop. However, the series insertion of the resistor results in dissipation of a large amount of power, from not only the high-frequency oscillatory current or the normal-mode current, but also the nonoscillatory motor current flowing through the resistor. Three NMF's, each of which consists of
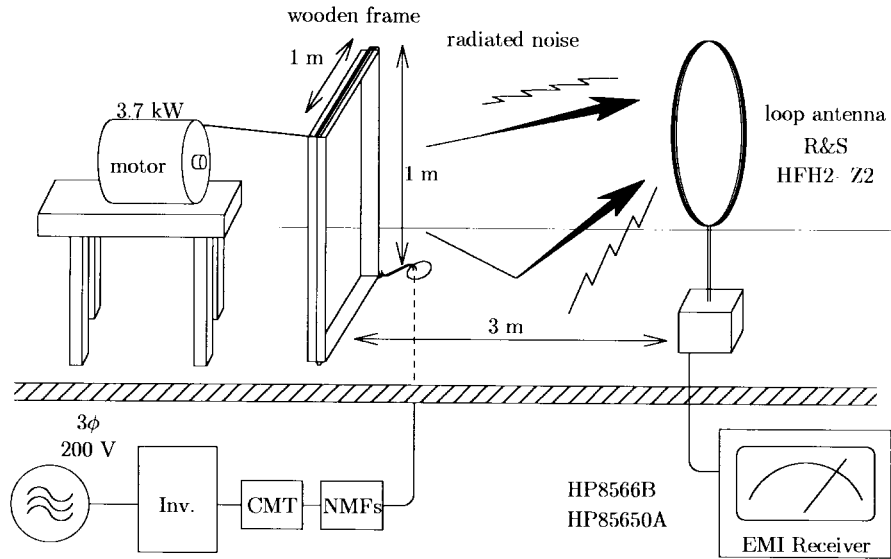
Fig. 13.   EMI measurement.

a resistor and an inductor, are connected between the inverter and motor terminals, so that only the high-frequency oscillatory current flows through the resistor, while the remaining inverter output current flows in the inductor. This justifies the series insertion of the resistor for damping of the normal-mode current oscillation.

Fig. 10 shows the normal-mode equivalent circuit, including the NMF's. The form of the normal-mode equivalent circuit is quite the same as that of the common-mode equivalent circuit shown in Fig. 6. This indicates that the method of designing the CMT [2] is applicable to the NMF's.

To damp the normal-mode current oscillation, the following condition should be satisfied:

$$2Z_{n0} < \frac{3}{2} R_f < \frac{1}{2} Z_{n\infty}. \tag{1}$$

Here,

$$Z_{n0} = \sqrt{\frac{L_n}{C_n}}$$
$$Z_{n\infty} = \sqrt{\frac{3}{2} \frac{L_f}{C_n}}. \tag{2}$$

Therefore, the normal-mode filter inductance is computed as 133 μH, because L_f should be larger than $16\frac{3}{2} L_n = 85$ μH. Fig. 11 shows an actual inductor used in the NMF. A resistor of 100 Ω is connected in parallel to the inductor. The cutoff frequency of the NMF is calculated by

$$\frac{R_f}{2\pi L_f} = 120 \text{ kHz}. \tag{3}$$

The NMF acts as a resistor of 100 Ω in a much higher frequency range than the cutoff frequency, while it acts as an inductor of 133 μH in a much lower frequency range.

Fig. 12 shows the experimental waveform of the inverter output current when connected with the NMF's. The peak value of the normal-mode current is reduced to 1 A, and the normal-mode current oscillation is perfectly damped by the NMF's.

VI. MEASUREMENT OF EMI

Fig. 13 shows a schematic diagram of the EMI measurement performed in a semi-anechoic chamber. The inverter, the CMT, and the NMF's, along with the EMI receiver, are located in the basement, directly underneath the semi-anechoic chamber, in order to measure only the EMI caused by the high-frequency oscillatory currents flowing in the grounding wire and the feeding wires between the inverter and motor terminals. All the wires are fixed along a wooden frame of 1 m $\times$ 1 m. The measurement is performed, based on the following four different wiring ways:

1) winding the three feeding wires and the grounding wire up into a bundle;
2) separating the ground wire from the feeding wires to form a nonnegligible circuit loop;
3) intentionally wiring the u-phase feeder incorrectly to form a nonnegligible circuit loop;
4) using a shielded three-core cable, the shielding conductor of which is used as the grounding wire.

Fig. 14 shows the tested induction motor and the wooden frame for experiment and measurement. The motor is put on a wooden desk. In wiring 1), the feeding wires and the grounding wire are fixed together along the upper and right sides of the wooden frame. In wiring 2) or 3), either the grounding wire or the u-phase feeding wire is fixed along the left and lower sides of the frame, thus, forming a circuit loop. In wiring 4), the shielded conductor used as the grounding wire is connected between the motor frame and the virtual grounding point.

Fig. 15 shows the measured result of radiated EMI in wiring 1), without the CMT and the NMF's. The radiated EMI does not exceed the limit value, although the common-mode and normal-mode currents flow together. The radiation is negligible because the magnetic fields produced by the currents cancel each other out.

Fig. 16 shows radiated EMI in wiring 2), without the CMT and the NMF's. Wiring 2) corresponds to the general wiring condition that the three-phase feeding wires are made up in
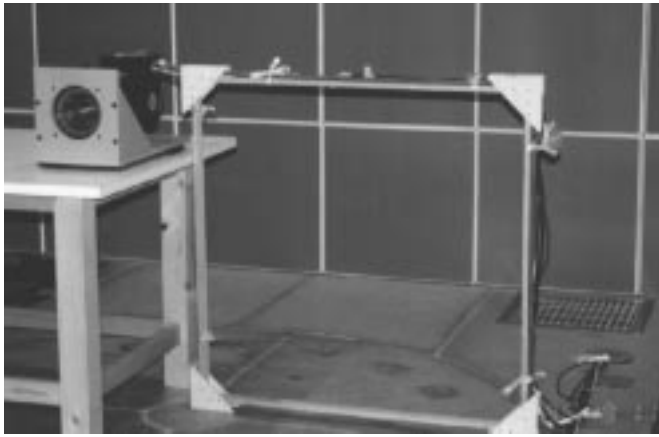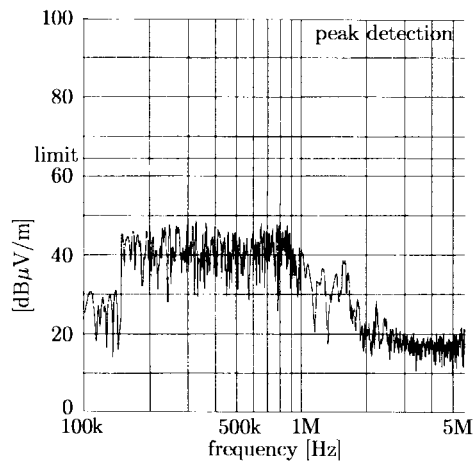
Fig. 14.   Measurement situation.

Fig. 16.   Radiated EMI [wiring 2)].

Fig. 15.   Radiated EMI [wiring 1)].

Fig. 17.   Radiated EMI [wiring 3)].

Fig. 18.   Radiated EMI [wiring 4)].

a bundle, while the motor frame is connected to a ground terminal through the grounding wire "separated" from the bundle. Hence, each phase of common-mode current flowing in the circuit loop formed by the feeding wires and the grounding wire can radiate EMI. However, the normal-mode current can hardly radiate EMI, although it flows in the feeding wires. Fig. 16 concludes that EMI in a range from 150 kHz–1 MHz exceeds the limit value by 15 dB.

Fig. 17 shows radiated EMI in wiring 3), without the CMT and the NMF's. The common-mode current and the normal-mode current flow in the u-phase wire, where the u-phase common-mode current is equal to 1/3 of the ground current. Therefore, the EMI produced by the common-mode current in the range from 150 kHz to 1 MHz is smaller than that of Fig. 16 by about 10 dB. The EMI produced by the normal-mode current has a peak around 1.5 MHz, and the peak value exceeds the limit value by 15 dB. The peak frequency coincides with the resonant frequency of the normal-mode equivalent circuit shown in Fig. 9. The measured results shown in the above three figures indicate that both the common-mode and normal-mode currents can radiate EMI. Minimizing the loop area formed by the feeding and/or grounding wires, however, is effective in reducing radiated EMI.
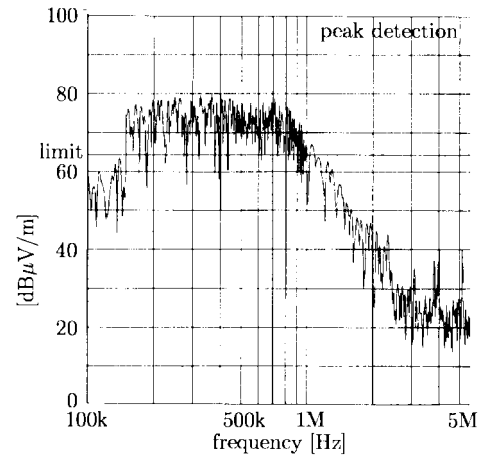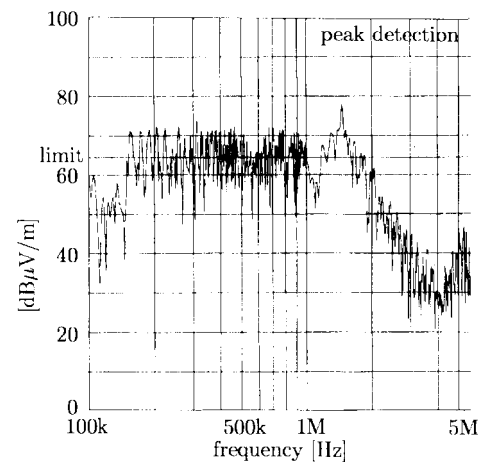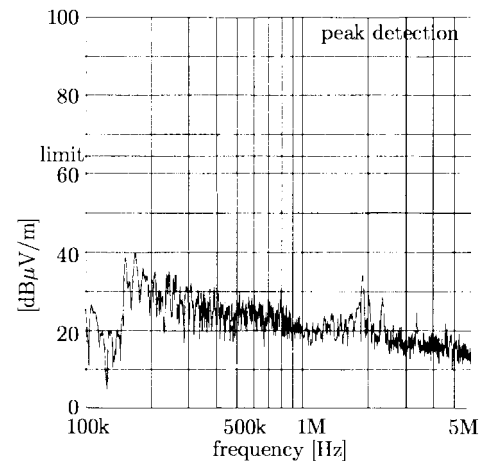
Fig. 18 shows radiated EMI in wiring 4), without the CMT and the NMF's. The result indicates that the use of the shielded three-core cable is more effective in suppressing the radiated EMI. Note that the shielded cable tends to have higher capacitance between each inner wire and the shielding conductor.
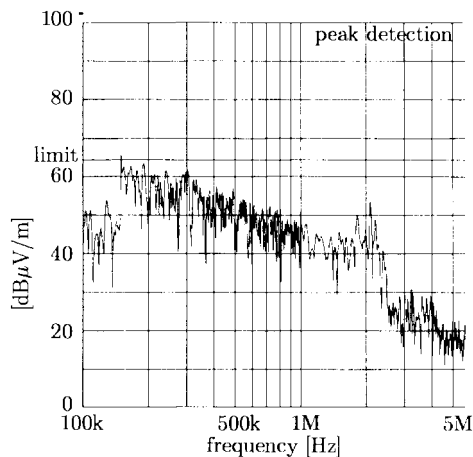
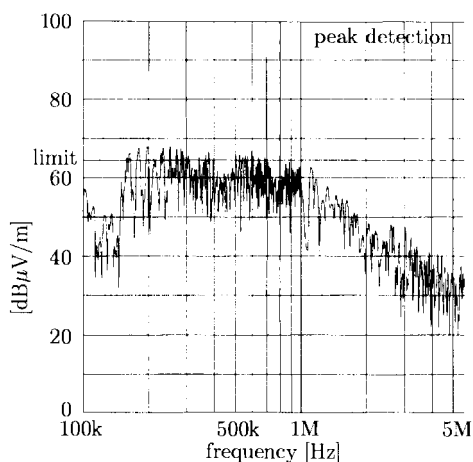Fig. 19. Radiated EMI with CMT and NMF's [wiring 2)].

Fig. 20. Radiated EMI with CMT and NMF's [wiring 3)].

Fig. 19 shows radiated EMI in wiring 2), with both the CMT and the NMF's. Compared with Fig. 16, the EMI in the range from 150 kHz to 1 MHz decreases by 20 dB, because the CMT can damp the common-mode current oscillation, as shown in Fig. 7. In this case, the EMI is suppressed within the limit value.

Fig. 20 shows radiated EMI in wiring 3), with both the CMT and the NMF's. The peak around 1.5 MHz in Fig. 17 perfectly disappears in Fig. 20, because of the excellent damping effect of the NMF's shown in Fig. 12.

VII. CONCLUSION

This paper has discussed the theoretical and experimental relationships between the EMI radiated throughout and the high-frequency oscillatory currents flowing through the stray capacitors inside an induction motor. The experimental results have led to the following conclusions.

- The motor model described in Fig. 2 is capable of dealing with both common-mode and normal-mode currents.
- The equivalent circuit for either the common-mode or normal-mode current is represented by an *LCR* series resonant circuit.

- Connecting both the CMT and the NMF's between the inverter and motor terminals is a practically viable and effective way, not only of damping the common-mode and normal-mode current oscillation, but also of reducing the EMI radiated by the current oscillation.
- The use of a shielded three-core cable is more effective in reducing radiated EMI than minimization of the loop area formed by the feeding wires and the grounding wire, although the oscillatory currents flow out from the inverter terminals.

The CMT and the NMF's can also reduce conducted EMI, improve insulation life, and reduce bearing current.

REFERENCES

[1] Y. Murai, T. Kubota, and Y. Kawase, "Leakage current reduction for a high-frequency carrier inverter feeding an induction motor," *IEEE Trans. Ind. Applicat.,* vol. 28, pp. 858–863, July/Aug. 1992.
[2] S. Ogasawara and H. Akagi, "Modeling and damping of high-frequency leakage currents in PWM inverter-fed AC motor drive systems," *IEEE Trans. Ind. Applicat.,* vol. 32, pp. 1105–1113, Sept./Oct. 1996.
[3] M. A. Jabbar and M. A. Rahman, "Radio frequency interference of electric motor and associated controls," *IEEE Trans. Ind. Applicat.,* vol. 27, pp. 27–31, Jan./Feb. 1991.
[4] G. Venkataramanan and D. M. Divan, "Pulse width modulation with resonant dc link converters," *IEEE Trans. Ind. Applicat.,* vol. 29, pp. 113–120, Jan./Feb. 1993.
[5] E. Zhong, S. Chen, and T. A. Lipo, "Improvement in EMI performance of inverter-fed motor drives," in *Conf. Rec. APEC 94,* 1994, vol. 2, pp. 608–614.
[6] S. Chen, T. A. Lipo, and D. Fitzgerald, "Modeling of motor bearing currents in PWM inverter drives," in *Proc. IEEE/IAS Annu. Meeting,* 1995, pp. 388–393.
[7] J. M. Erdman, R. J. Kerkman, D. W. Schlegel, and G. L. Skibinski, "Effect of PWM inverters on AC motor bearing currents and shaft voltages," *IEEE Trans. Ind. Applicat.,* vol. 32, pp. 250–259, Mar./Apr. 1996.
[8] B. Heller and A. Veverka, *Surge Phenomena in Electrical Machines.* London, U.K.: Iliffe Books, 1968.
[9] R. E. Pretorius and A. J. Eriksson, "A basic guide to rc surge suppression on motors and transformers," *Trans. S. Africa Inst. Electr. Eng.,* pp. 201–209, Aug. 1980.
[10] B. K. Bose, "Power electronics and motion control—Technology status and recent trends," *IEEE Trans. Ind. Applicat.,* vol. 29, pp. 902–909, Sept./Oct. 1993.
[11] A. von Jouanne, D. Rendusara, P. Enjeti, and W. Gray, "Filtering technique to minimize the effect of long motor leads on PWM inverter fed AC motor drive systems," in *Proc. IEEE/IAS Annu. Meeting,* 1995, pp. 37–44.

Satoshi Ogasawara (A'87–M'93–SM'97) was born in Kagawa Prefecture, Japan, in 1958. He received the B.S., M.S., and Dr.Eng. degrees in electrical engineering from Nagaoka University of Technology, Niigata, Japan, in 1981, 1983, and 1990, respectively.

From 1983 to 1992, he was a Research Associate at the Nagaoka University of Technology. Since 1992, he has been with the Department of Electrical Engineering, Okayama University, Okayama, Japan, where he is currently an Associate Professor. His research interests are ac motor drives systems and static power converters.

Dr. Ogasawara is a member of the Institute of Electrical Engineers of Japan.

Hideki Ayano was born in Okayama Prefecture, Japan, in 1973. He received the B.S. and M.S. degrees in electrical and electronic engineering from Okayama University, Okayama, Japan, in 1995 and 1997, respectively.

In 1997, he joined the Power and Industrial Systems Research and Development Department, Hitachi, Ltd., Hitachi, Japan. His research interest is EMI produced by inverters.

Hirofumi Akagi (M'87–SM'94–F'96) was born in Okayama-city, Japan, in 1951. He received the B.S. degree from the Nagoya Institute of Technology, Nagoya, Japan, in 1974 and the M.S. and Ph.D. degrees from the Tokyo Institute of Technology, Tokyo, Japan, in 1976 and 1979, respectively, all in electrical engineering.

In 1979, he joined the Department of Electrical Engineering, Nagaoka University of Technology, Niigata, Japan, as an Assistant Professor, later becoming an Associate Professor. In 1987, he was a Visiting Scientist at Massachusetts Institute of Technology, Cambridge, for ten months. Since 1991, he has been a Full Professor in the Department of Electrical Engineering, Okayama University, Okayama, Japan. From March to August of 1996, he was a Visiting Professor at the University of Wisconsin, Madison, and the Massachusetts Institute of Technology. His research interests include ac motor drives, high-frequency resonant inverters for induction heating and corona discharge treatment, and utility applications of power electronics such as active filters, static var compensators, and FACTS devices.

Dr. Akagi has received six IEEE Industry Applications Society Prize Paper Awards, including the First Prize Paper Award in the IEEE TRANSACTIONS ON INDUSTRY APPLICATIONS in 1991.